

Indoor Direction Diversity at 5.8 GHz

Robert J. Achatz
Yeh Lo
Elizabeth E. Pol



U.S. DEPARTMENT OF COMMERCE
William M. Daley, Secretary

Larry Irving, Assistant Secretary
for Communications and Information

July 1998

CONTENTS

	Page
ABSTRACT	1
1. INTRODUCTION	1
2. MEASUREMENT DESCRIPTION	2
2.1 Equipment.....	2
2.2 Location.....	5
2.3 Procedure.....	5
3. ANALYSIS DESCRIPTION	8
3.1 Antenna Diversity Technique.....	8
3.2 Example.....	10
4. RESULTS.....	11
4.1 Mobile Station Antenna Delay Spreads	11
4.2 Diversity Algorithm Delay Spreads	16
5. CONCLUSION	17
6. REFERENCES.....	18
APPENDIX: MEASURED IMPULSE RESPONSES	19

INDOOR DIRECTION DIVERSITY AT 5.8 GHz

Robert J. Achatz¹, Yeh Lo¹, Elizabeth E. Pol²

Complex impulse response measurements of a warehouse building were made at 5.8 GHz with a sliding correlator channel probe. These measurements were made with vertically and horizontally polarized directional antennas so performance improvement due to polarization- and direction-diversity could be evaluated. Improvement in performance was determined by changes in the radio channel's delay spread. Performance improved with direction diversity; however, adding polarization diversity yielded little improvement over direction diversity alone.

Key words: complex impulse response measurements; direction diversity; polarization diversity; indoor propagation; delay spread

1. INTRODUCTION

Signals transmitted indoors are reflected, diffracted, and scattered by a building's walls, floor, ceiling, and furnishings. These phenomena cause the transmitted signal to arrive at the receiver via two or more paths with unique delays, direction-of-arrivals, and polarizations. The delayed signals degrade receiver performance by causing intersymbol interference (ISI). Intersymbol interference can be reduced with direction diversity by passing signals arriving from a desired direction and attenuating signals arriving from all other directions [1]. Direction/polarization diversity, which adds polarization discrimination to direction diversity, may reduce ISI further [2,3].

These diversity measures are important for two reasons. First, decreasing ISI at the antenna minimizes the need for traditional multipath mitigation techniques such as equalization, which may require high-speed signal processing, and spread spectrum echo cancellation, which increases radio spectrum requirements. Second, the directional antennas used with these diversity measures become smaller as frequency increases. This helps to alleviate spectral congestion at lower frequencies by making higher frequencies more attractive for applications where compactness is desirable.

The Institute for Telecommunication Sciences (ITS) performed complex impulse response measurements at 5.8 GHz in a warehouse building with vertically and horizontally polarized, directional antennas in order to determine the effectiveness of direction- and direction/polarization-diversity. Delay spread, derived from the complex impulse response measurements, was used to quantify the improvement in performance due to these antenna diversity techniques.

¹ The authors are with the Institute for Telecommunication Sciences, National Telecommunications and Information Administration, U.S. Department of Commerce, Boulder, CO 80303.

² The author was with the Institute for Telecommunication Sciences when this work was done.

2. MEASUREMENT DESCRIPTION

In this section the equipment used to measure the complex impulse response is described, the warehouse building where the measurements were conducted is depicted, and the measurement procedure is explained.

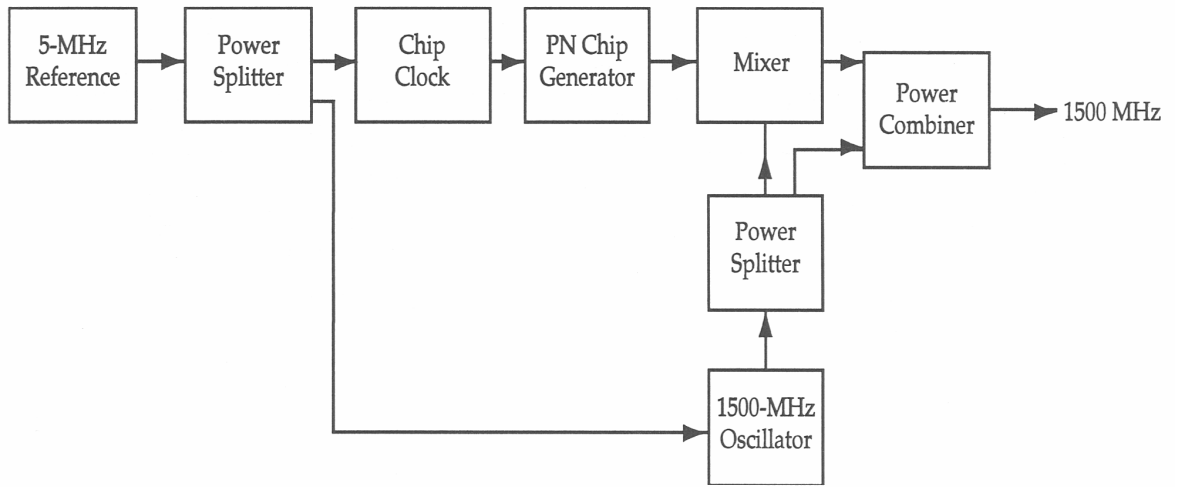
2.1 Equipment

The ITS sliding correlator channel probe [4] was used to measure the complex impulse responses. Figures 1 and 2 describe the channel probe's transmitter and receiver, respectively. Pseudorandom noise (PN) sequences, 127 "chips" in length, are generated at a rate of 100 million chips/s in the transmitter modulator. The chips bi-phase modulate a 1.5-GHz carrier to produce a signal that is up-converted to the 5.8-GHz carrier frequency. The transmitter's final amplifier delivers 23 dBm of signal power to the antenna.

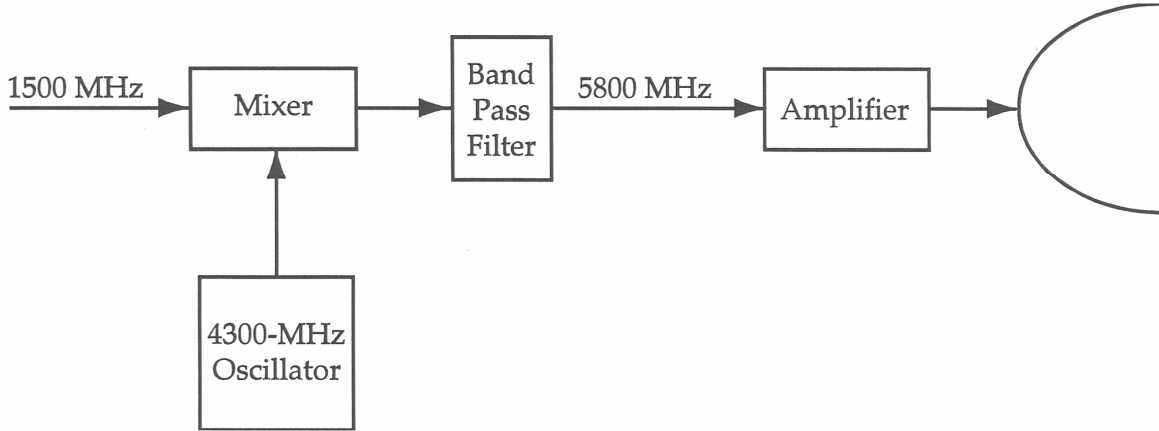
The receiver downconverts the signal to 1.5 GHz, quadrature demodulates it into baseband inphase and quadrature channels, and correlates a copy of the transmitted PN sequence with each channel. The variable attenuator before the receiver's low-noise amplifier is adjusted to avoid amplifier saturation. The recording level of the digital audio tape recorder is also adjusted to maximize recording dynamic range.

The receiver has a 9-dB noise figure, a dynamic range of approximately 35 dB, a time delay resolution of 10 ns, and an unambiguous time delay range of 1.27 μ s. The 5-MHz oscillators in the transmitter and receiver are phase locked to each other by a signal transmitted over a coaxial cable. The receiver's chip rate is slightly offset from the transmitter's chip rate so that all transmission time delays up to the unambiguous time delay range are periodically measured.

The receiver was mounted in a fixed rack while the transmitter was mounted on a cart with wheels; thus, in this report, the receiver is called the fixed station (FS) and the transmitter the mobile station (MS). The antenna height at the FS and MS was 2.1 m and 1.2 m, respectively. The antennas used by the FS and MS are summarized in Table 1 and 2. Mobile station horn A and B antennas are identical; however, horn B was rotated 90° so that it would be horizontally polarized.

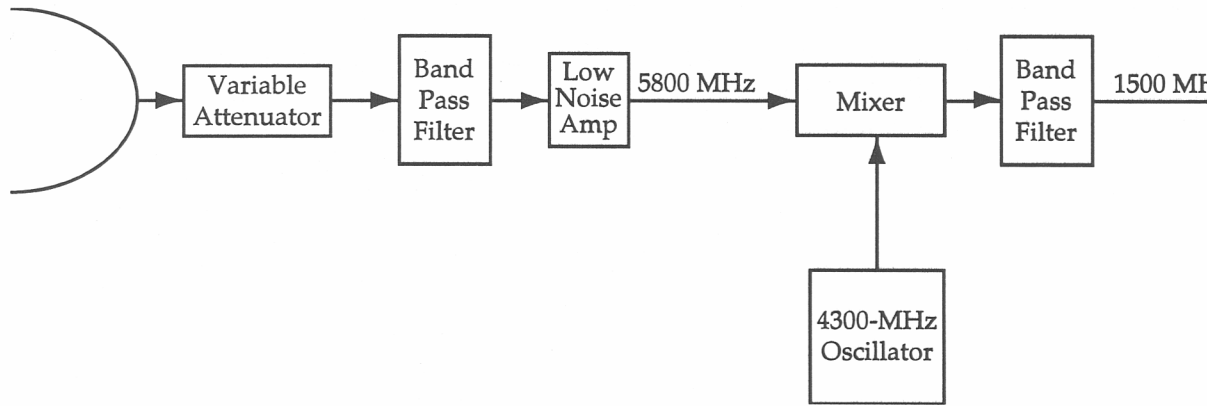


(a)

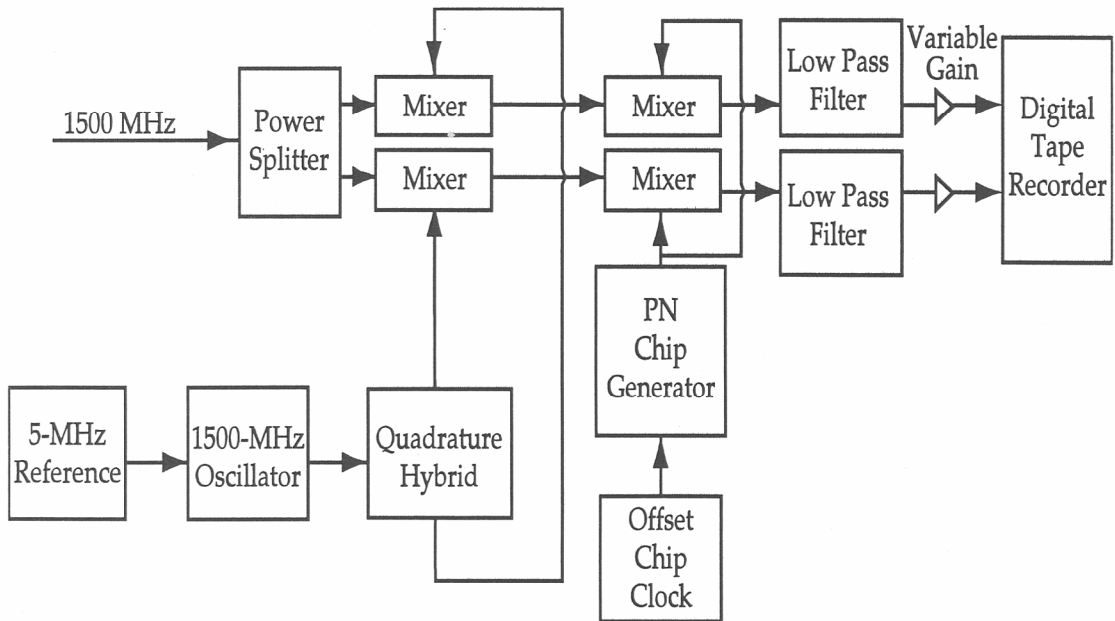


(b)

Figure 1. Channel probe transmitter: a) modulator and b) up-converter.



(a)



(b)

Figure 2. Channel probe receiver: a) down-converter and b) demodulator.

Table 1. Fixed Station Antennas

Antenna Type	Biconical	Log Periodic
Gain (dBi)	3	8
Polarization	vertical	vertical
Vertical 3-dB Beamwidth	60°	60°
Horizontal 3-dB Beamwidth	360°	60°

Table 2. Mobile Station Antennas

Antenna Type	Biconical	Horn A	Horn B
Gain (dBi)	3	15	15
Polarization	vertical	vertical	horizontal
Vertical 3-dB Beamwidth	60°	29°	22°
Horizontal 3-dB Beamwidth	360°	22°	29°

2.2 Location

A warehouse shelving area, depicted in Figure 3, was measured. The shelving area is located at the end of a large building on the Department of Commerce campus in Boulder, Colorado. Three of the shelving area's sides are outside walls while the fourth is open to the rest of the building. The walls and floor are made of concrete and the roof is made of galvanized steel panels. The walls are approximately 22 m long and the roof is roughly 6 m high.

The shelving area contains 8 large metal shelves, 3 m high and 2 m wide, that hold boxes of office supplies and other miscellaneous goods. Two large shelves extend along the back and side wall. The remaining 6 large shelves are located adjacent to paths 1 through 6. The shelf next to path 6, which separates the shelving area from the rest of the building, holds a large quantity of metal stock (e.g., brass rods) used to manufacture specialized scientific apparatus.

2.3 Procedure

Four measurement configurations, shown in Figure 4, were used in the experiment. Each measurement configuration has a unique FS antenna type, FS azimuth, and FS location as summarized in Table 3. Although the transmitter was moved from one MS location to another, the measurements at each MS location were collected while the transmitter was stationary. Thirteen

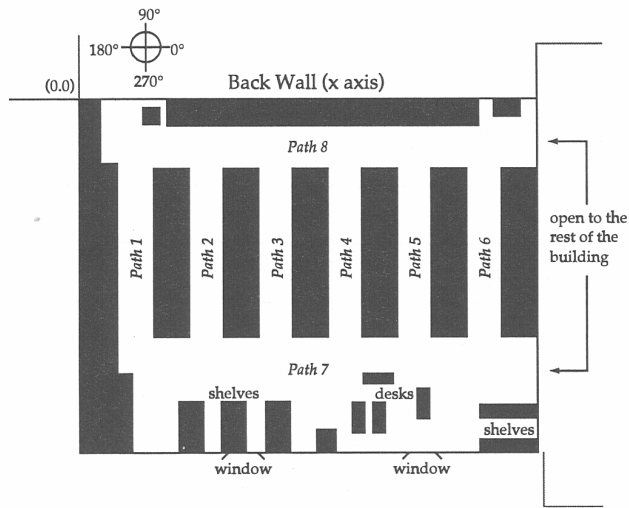


Figure 3. Warehouse floor plan.

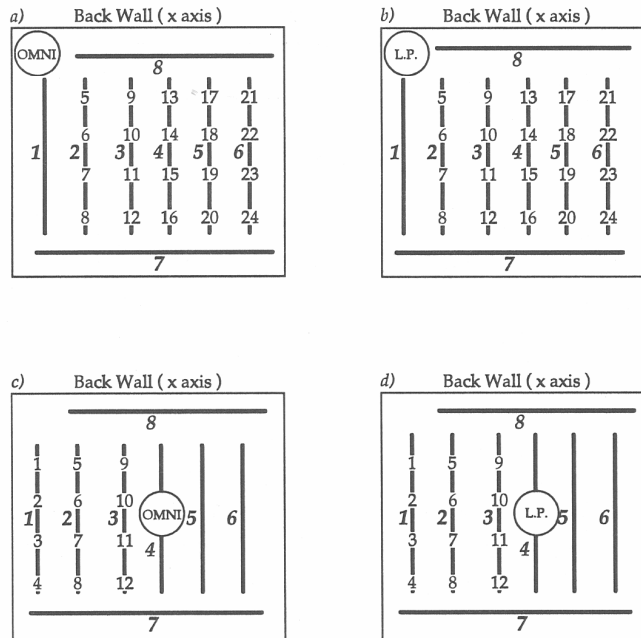


Figure 4. Measurement configurations where: a) is configuration 1, b) is configuration 2, c) is configuration 3, and d) is configuration 4. Numbers on paths are the mobile station locations, bold numbers are the path number, and the OMNI and LP labels refer to the fixed station biconical and log periodic antennas, respectively.

unique MS measurements identified by MS antenna type and MS antenna azimuth were collected at each MS location. The first MS measurement used the biconical antenna while the last twelve varied horn azimuth and polarization as summarized in Table 4. Approximately 100 complex impulse responses were collected for each MS measurement.

Table 3. Measurement Configurations

. Configuration	FS Antenna Type	FS Antenna Azimuth	FS Antenna Location
1	Biconical	Omnidirectional	Comer
2	Log Periodic	300°	Comer
3	Biconical	Omnidirectional	Center
4	Log Periodic	180°	Center

Table 4. Mobile Station Measurements

MS Measurement	MS Antenna Type	MS Antenna Azimuth
1	Biconical	Omnidirectional
2	Horn A	0°
3	Horn B	0°
4	Horn A	60°
5	Horn B	60°
6	Horn A	120°
7	Horn B	120°
8	Horn A	180°
9	Horn B	180°
10	Horn A	240°
11	Horn B	240°
12	Horn A	300°
13	Horn B	300°

3. ANALYSIS DESCRIPTION

In this section, our antenna diversity techniques are described and an example MS location is chosen to illustrate how the diversity algorithms were implemented.

3.1 Antenna Diversity Technique

The multipath channel's effect on the transmitted signal is dependent upon the transmitted signal's bandwidth. The multipath channel is "frequency flat" if its transfer function's amplitude and group delay are constant over frequencies in the signal's bandwidth. Conversely, the multipath channel is "frequency selective" if its transfer function's amplitude or group delay changes over the same frequencies. The frequency-flat channel transfer function degrades reception by attenuating the signal whereas the frequency-selective channel degrades reception primarily by introducing ISI. In this study we were concerned only with the frequency-selective channel effects; we therefore assumed that signal attenuation was not limiting the radio link's performance and used the antenna diversity algorithm to select the antenna whose direction or direction/polarization minimized the ISI.

Our first task was to identify an algorithm for quantifying ISI using the measured impulse responses. We considered two algorithms. The first algorithm quantified ISI with the minimum mean-squared-error (MSE) between the signal distorted by the frequency-selective channel and the same signal that had been attenuated, phase shifted, and time delayed by some optimum A , θ , and τ respectively:

$$\xi^2 = \langle (s(t) * h(t) - Ae^{j\theta} s(t - \tau)) \rangle^2 \quad (1)$$

where $s(t)$ is the complex baseband representation of the signal and $h(t)$ is the measured complex impulse response [5]. The second algorithm computed the "delay spread" of $h(t)$, a measure that corresponds to signal energy dispersion in time. Since ISI is defined as the amount of extraneous energy from one symbol's time interval that interferes with the energy of a symbol in another time interval, we assumed that ISI is correlated to delay spread [6]. We chose the delay spread calculation for this study because it does not require computation of an optimum A , θ , and τ .

There are several measures of impulse response delay spread [7,8]. In this study we used the area moment of inertia of $|h(t)|^2$. Analytically, we let

$$p(t) = |h(t)|^2, \quad (2)$$

normalized $p(t)$ to $P(t)$ with unit area

$$P(t) = \frac{p(t)}{\int_{t=0}^{\tau_{\max}} p(t) dt}, \quad (3)$$

determined the mean delay m of $P(t)$

$$m = \int_{t=0}^{\tau_{\max}} tP(t)dt, \quad (4)$$

and calculated the square-root area moment of inertia σ of $P(t)$

$$\sigma = \sqrt{\int_{t=0}^{\tau_{\max}} (t-m)^2 P(t)dt}. \quad (5)$$

Throughout these calculations the value of $P(t)$ was set to zero when it was less than 20 dB below the maximum $P(t)$ amplitude to minimize the effects of noise. The function $p(t)$ was averaged over time to remove additive noise. However, since the transmitter and receiver were stationary during each measurement, the data does not represent a “spatially averaged power delay profile” that characterizes the MS location as in [9] and therefore was not used to predict the bit error rate of radios operating in Gaussian, wide-sense stationary, uncorrelated scattering, channels as described in [10].

Our second task was to define the direction- and direction/polarization-diversity algorithms. The direction diversity algorithm assumes the radio link has a vertically polarized, biconical or log periodic antenna at one end of the radio link and an array of vertically polarized, equally spaced in azimuth, horn antennas at the other. The direction diversity algorithm selects the horn antenna azimuth with the smallest delay spread. In our study the direction diversity algorithm selects the smallest horn A antenna delay spread from MS measurements 2, 4, 6, 8, 10, or 12.

The direction/polarization diversity algorithm assumes the radio link has a vertically polarized, biconical or log periodic antenna at one end of the radio link and an array of vertically and horizontally polarized, equally spaced in azimuth, horn antennas at the other. The direction/polarization diversity algorithm selects the horn antenna azimuth and polarization with the smallest delay spread. In our study the direction/polarization diversity algorithm selects the smallest horn A or horn B antenna delay spread from MS measurements 2 through 13.

The no-diversity case assumes the radio link has a vertically polarized, biconical or log periodic antenna at one end of the radio link and a vertically polarized, biconical antenna at the other. In our study the no-diversity case always uses the delay spread in MS measurement 1.

3.2 Example

Table 5 shows the delay spreads for configuration 3, MS location 9, for each of the MS measurements. The measured $p(t)$ functions used to compute the delay spreads are shown in Appendix A. The MS antenna delay spreads used in the antenna diversity algorithm are listed in Table 6. The horn A and horn B antenna delay spreads reported in Table 6 refer to the horn's smallest delay spread over all measured azimuths. For this example, both horn antennas have lower delay spreads than the biconical antenna; however, the vertically polarized horn A antenna has a lower delay spread than the horizontally polarized horn B antenna.

The diversity algorithm delay spreads for this example are summarized in Table 7. The no-diversity case corresponds to the biconical MS antenna delay spread, the direction diversity case corresponds to the minimum horn A MS antenna delay spread, and the direction/polarization diversity case corresponds to the minimum horn A or horn B MS antenna delay spread.

Table 5. Delay Spreads for Configuration 3, MS Location 9

MS Measurement	MS Antenna Type	MS Antenna Azimuth	Delay Spread (ns)
1	Biconical	Omnidirectional	25.9
2	Horn A	0°	23.7
3	Horn B	0°	22.9
4	Horn A	60°	08.0
5	Horn B	60°	22.1
6	Horn A	120°	24.1
7	Horn B	120°	18.1
8	Horn A	180°	25.5
9	Horn B	180°	22.7
10	Horn A	240°	19.9
11	Horn B	240°	32.0
12	Horn A	300°	27.8
13	Horn B	300°	30.3

Table 6. MS Antenna Delay Spreads for Configuration 3, MS Location 9

MS Antenna Type	Biconical	Horn A	Horn B
MS Measurement	1	4	7
Delay Spread (ns)	25.9	8.0	18.1

Table 7. Diversity Algorithm Delay Spreads for Configuration 3, MS Location 9

Diversity	No-diversity	Direction	Direction/ polarization
MS Measurement	1	4	4
Delay Spread (ns)	25.9	8.0	8.0

4. RESULTS

The MS antenna delay spreads for all configurations and MS locations are presented. Cumulative distributions of diversity algorithm delay spreads are shown for all configurations to statistically quantify the effectiveness of the diversity measures.

4.1 Mobile Station Antenna Delay Spreads

Using the method described above, MS antenna delay spreads were computed for all configurations and MS locations. The results, which correspond to the example results in Table 6, are shown in Figures 5 through 8. The figures show that the vertically polarized horn A antenna had a lower delay spread than the biconical antenna at most MS locations. Exceptions to this include configuration 1, MS location 8; and configuration 2, MS location 23. Vertically polarized horn A antenna delay spreads were also lower than horizontally polarized horn B antenna delay spreads at most MS locations. Exceptions to this include configuration 1, MS locations 11, 14, and 15; and configuration 2, MS locations 10, 11, 14, and 17. The biconical antenna delay spread of configuration 1, MS location 10 was approximately 70 ns, which exceeds the graph's vertical scale.

Delay spreads for MS locations 13-24 are generally higher than delay spreads for MS locations 1-12. This trend corresponds to observations [4] that delay spread typically increases with path distance.

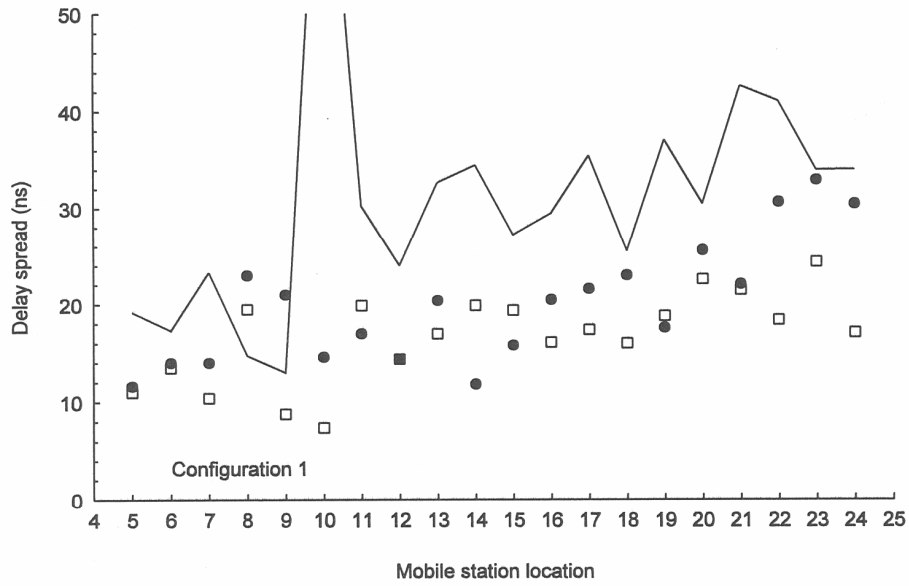


Figure 5. Delay spreads for configuration 1. Solid line, square, and circle represent mobile station with biconical, horn A, and horn B antennas, respectively.

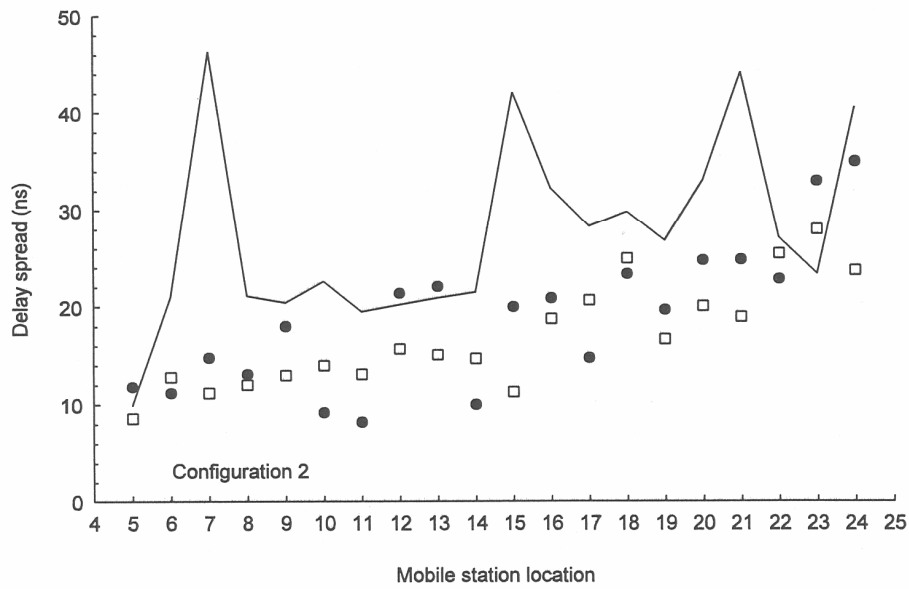


Figure 6. Delay spreads for configuration 2. Solid line, square, and circle represent mobile station with biconical, horn A, and horn B antennas, respectively.

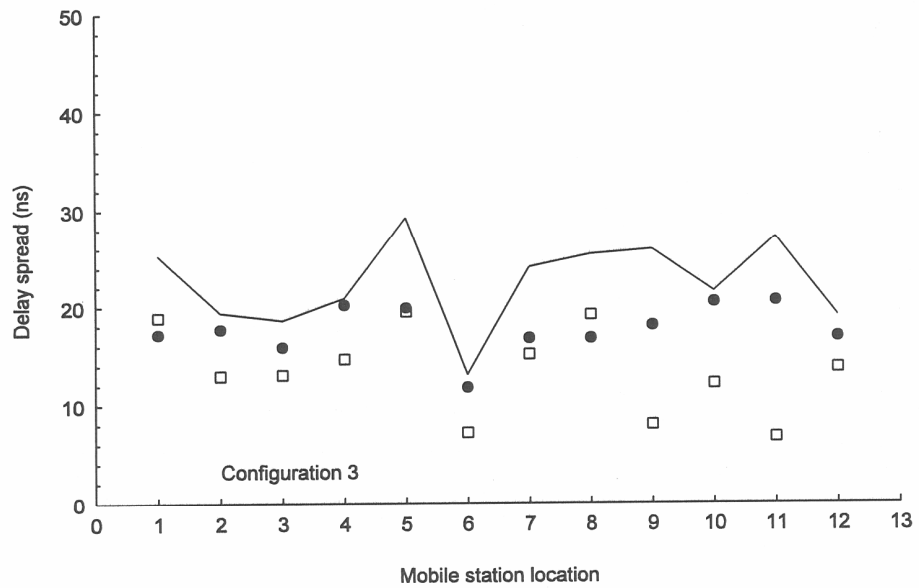


Figure 7. Delay spreads for configuration 3. Solid line, square, and circle represent mobile station with biconical, horn A, and horn B antennas, respectively.

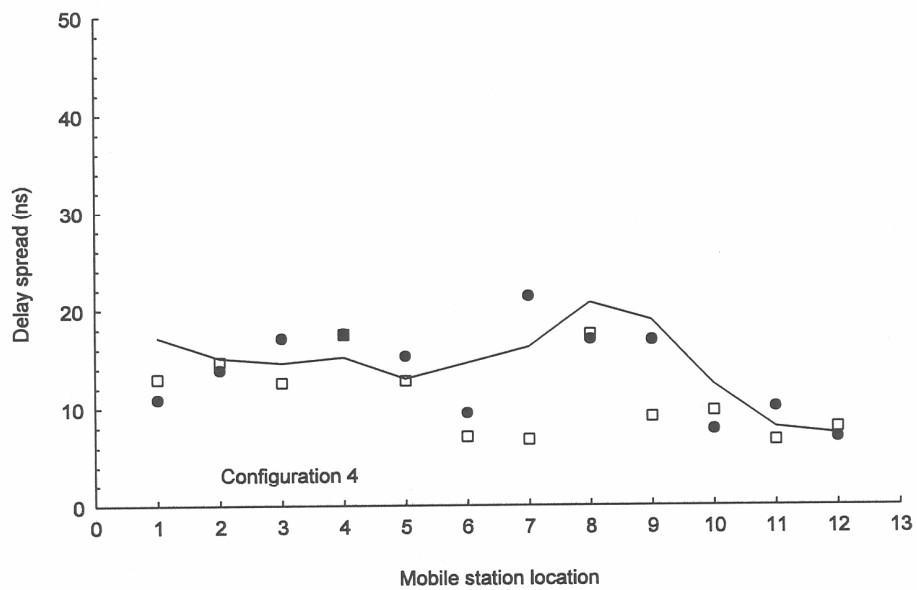


Figure 8. Delay spreads for configuration 4. Solid line, square, and circle represent mobile station with biconical, horn A, and horn B antennas, respectively.

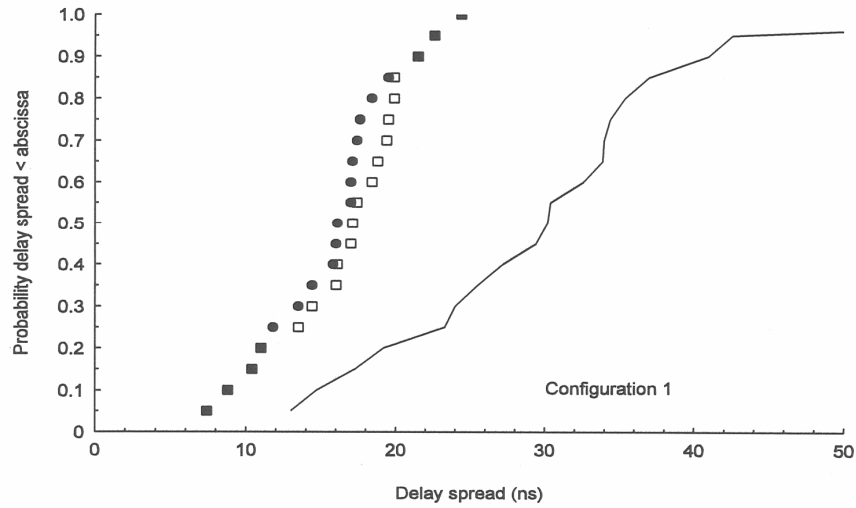


Figure 9. Cumulative distribution of diversity algorithm delay spreads for configuration 1. Solid line, square, and circle represent mobile station with no diversity, direction diversity, and direction/polarization diversity respectively.

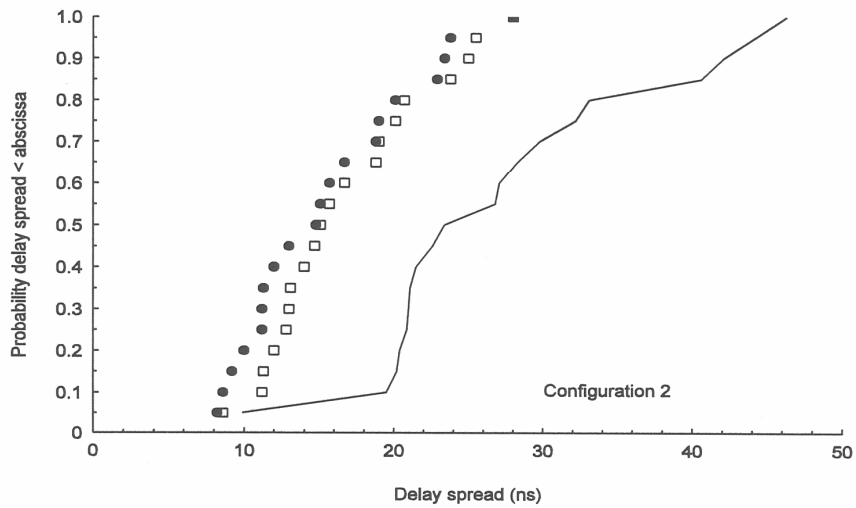


Figure 10. Cumulative distribution of diversity algorithm delay spreads for configuration 2. Solid line, square, and circle represent mobile station with no diversity, direction diversity, and direction/polarization diversity respectively.

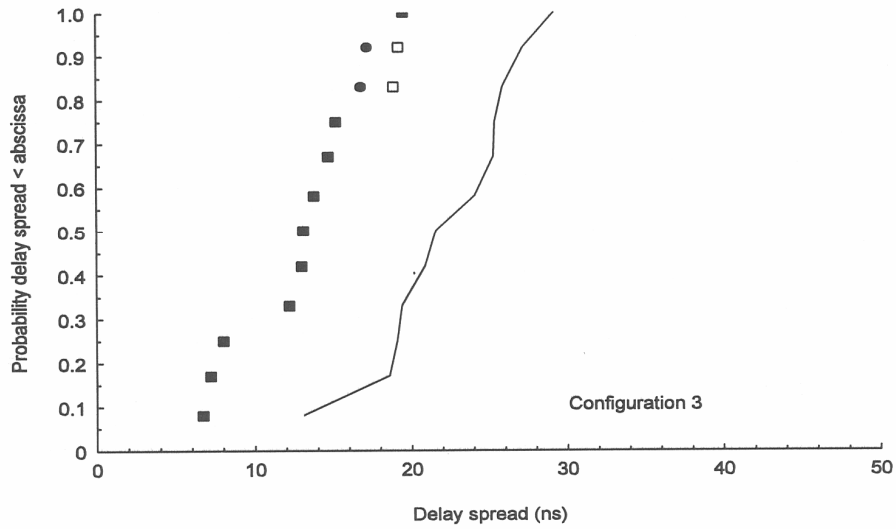


Figure 11. Cumulative distribution of diversity algorithm delay spreads for configuration 3. Solid line, square, and circle represent mobile station with no diversity, direction diversity, and direction/polarization diversity respectively.

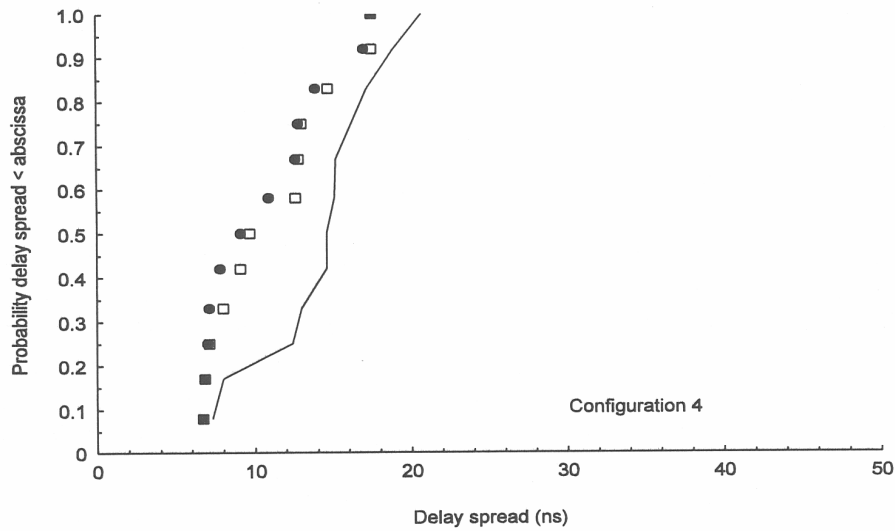


Figure 12. Cumulative distribution of diversity algorithm delay spreads for configuration 4. Solid line, square, and circle represent mobile station with no diversity, direction diversity, and direction/polarization diversity respectively.

Table 8. Maximum Delay Spreads for 50% of Mobile Station Locations

Configuration	Diversity Delay Spreads (ns)		
	No-diversity	Direction	Direction/ Polarization
1	30	17	16
2	23	15	15
3	22	13	13
4	15	9	9

Table 9. Maximum Delay Spreads for 90% of Mobile Station Locations

Configuration	Diversity Delay Spreads (ns)		
	No-diversity	Direction	Direction/ Polarization
1	42	22	22
2	42	25	23
3	27	19	17
4	18	17	17

4.2 Diversity Algorithm Delay Spreads

Diversity algorithm delay spreads, which correspond to the example results in Table 7, for each configuration and MS location can be obtained from Figures 5 through 8. The no-diversity delay spread is the same as the biconical MS antenna delay spread, direction diversity delay spread is the smallest horn A antenna delay spread, and direction/polarization diversity delay spread is the smallest of the horn A and horn B antenna delay spreads. Figures 9 through 12 show the cumulative distribution functions (CDF's) of the diversity algorithm delay spreads. The CDF's clearly show that direction- and direction/polarization-diversity lower the delay spread from no-diversity values. The CDF's also show that adding polarization diversity to direction diversity does not improve performance significantly. Tables 8 and 9 summarize the maximum delay spreads for 50% and 90% of MS locations.

5. CONCLUSION

The results of this study indicate that direction diversity, implemented at one end of a 5.8-GHz indoor radio link, decreases the delay spread relative to the delay spread measured without diversity. These results were true for all four combinations of fixed station antenna types, azimuths, and locations depicted in Table 3. Figures 5 through 8 show that the horizontally and vertically polarized horn antennas have lower mobile station antenna delay spreads than the biconical antenna. The statistics of diversity algorithm delay spread, independent of mobile station location, are depicted in Figures 9 through 12. These statistics show that reductions in median direction diversity delay spread ranged from approximately 35% to 45% depending on the configuration. Adding polarization diversity to direction diversity decreased the delay spread in a small number of mobile station locations; however, these locations had little impact on the 50% and 90% quantiles of delay spread statistics summarized in Tables 8 and 9.

The decrease in delay spread due to direction and direction/polarization diversity shows that arrays of directional antennas can be used to reduce intersymbol interference in a frequency-selective multipath channel. Radio link engineers know that propagation losses, which increase with frequency, can be compensated for by using higher gain, directional antennas. They also know that directional antenna size decreases as frequency increases if gain is held constant. These attributes of directional antennas combined with the results of this study indicate that wideband, indoor radio links using directional diversity may be well-suited to higher microwave frequencies bands.

6. REFERENCES

- [1] J.E. Mitzlaff, "Radio propagation and anti-multipath techniques in the WIN environment," *IEEE Network Magazine*, pp. 21-26, Nov. 1991.
- [2] T.S. Rappaport and D.A. Hawbaker, "Wide-band microwave propagation parameters using circular and linear polarized antennas for indoor wireless channel," *IEEE Trans. Commun.*, pp. 240-245, Feb. 1992.
- [3] D.C. Cox, "Cross-polarization coupling measured for 800 MHz radio transmission in and around houses and large buildings," *IEEE Trans. Ant. Prop.*, pp. 83-87, Jan. 1986.
- [4] P.B. Papazian, Y. Lo, E.E. Pol, M.P. Roadifer, T.G. Hoople, and R.J. Achatz, "Wideband propagation measurements for wireless indoor communication," NTIA Report 93-292, Jan. 1993.
- [5] M.C. Jeruchim, P. Balaban, and K.S. Shanmugan, *Simulation of Communication Systems*, New York: Plenum Press, 1992, pp. 479-486.
- [6] G.A. Hufford, "A characterization of the multipath in the HDTV channel," *IEEE Trans. Broadcasting*, pp. 252-255, Dec. 1992.
- [7] G.A. Hufford, R.W. Hubbard, L.E. Pratt, J.E. Adams, and S.J. Paulson, "Wide band propagation measurements in the presence of forests," U.S. Army Communications-Electronics Command Report CECOM 82-CS029-F, Jan. 1982.
- [8] J.D. Parsons, *The Mobile Radio Propagation Channel*, London: Pentec Press, 1992, pp. 162-188.
- [9] D.M. Devasirvatham, "Multipath time delay spread in the digital portable radio environment" *IEEE Commun. Magazine*, pp. 13-21, Jun. 1987.
- [10] J.C-I Chuang, "The effects of time delay spread on portable radio communications channels with digital modulation," *IEEE J. Selected Areas Commun.*, pp. 879-889, Jun. 1987.